J Mater Sci (2006) 41:5302–5309
DOI 10.1007/s10853-006-0255-9

Epitaxial growth of $Sr_x\ Ba_{1-x}\ Nb_2\ O_6$ (SBN) thin films on Pt coated MgO substrates: the determining control of platinum crystallographic orientation

M. Cuniot-Ponsard · J. M. Desvignes · A. Bellemain

Received: 22 February 2005 / Accepted: 7 October 2005 / Published online: 6 June 2006

Abstract The growth of (001) oriented $Sr_x\ Ba_{1-x}\ Nb_2\ O_6$ (SBN:x) thin films on MgO single crystals substrates has focused attention due to its potential application to integrated signal waveguiding and electro-optic processing. This paper addresses the possible insertion of a platinum bottom electrode to implement the electro-optic effect, and examines the influence of Pt orientation on the subsequent growth of SBN thin films deposited by R.F. magnetron sputtering. We have first investigated the optimal sputtering conditions of a (001) Pt oriented growth. Experimental evidence is provided for an orientation switching temperature sensitive to R.F. power but insensitive to deposition rate which suggests that kinetic phenomena are not involved in the orientation development of Pt films. Seeding the MgO substrate with Fe, Cu or Cr inhibits the competitive (111) Pt growth without modifying the optimal temperature for (001) growth. Annealing at a temperature sufficient to crystallise the top SBN film causes a drastic evolution of the initial (111) and (001) Pt volume fractions, making particularly critical the deposition conditions for a final dominant (001) Pt texture on unseeded substrates. The (001) oriented growth of SBN is shown to occur exclusively on (001) Pt crystallites stable against subsequent annealing steps. As a final result, (001) SBN films have been obtained epitaxial on both Pt coated and not coated (001) MgO substrates. They display two in-plane orientations mirror symmetric ($\pm\alpha$) to the axis of (001) MgO, with α shifted from 31° to 18° by (001) Pt coating.

M. Cuniot-Ponsard (✉) · J. M. Desvignes · A. Bellemain
Laboratoire Charles Fabry de l'Institut d'Optique, UMR 8501 du C.N.R.S. et de l'Université Paris Sud, Bât 503, Centre Scientifique, 91403 Orsay Cedex, France
e-mail: mireille.cuniot@iota.u-psud.fr

Introduction

Strontium barium niobate ($Sr_x\ Ba_{1-x}Nb_2O_6$ or SBN:x) is an attractive ferroelectric material which has been widely studied for holographic recording and optical processing. It exhibits one of the largest known linear electro-optic coefficients ($r_{33} \approx 1300$ pm V^{-1} for SBN:75), nearly two orders of magnitude larger than that of the primary electro-optic material $LiNbO_3$. The growth of (001) oriented SBN:x thin films on MgO single crystal substrates, which are of lower refractive index, has focused attention due to its potential application to integrated signal waveguiding and electro-optic processing. The oriented growth (001) SBN//(001) MgO has been reported from various deposition techniques including Metal Organic Chemical Vapor Deposition (MO-CVD) [1], Pulsed Laser Deposition (PLD) [2], Plasma Enhanced-CVD [3], sol-gel synthesis [4], combination of sol-gel and PLD [5], and R.F. sputter deposition [6].

Implementation of the electro-optic Pockels effect requires bottom and top electrodes. Among the possible conductive materials to be deposited on (001) MgO, platinum has been extensively studied for devices with ferroelectric, magneto-resistive, or magneto-optic applications, due to its chemical stability at high temperatures. Whatever deposition technique the authors used to prepare Pt thin films onto (001) MgO, the two orientations (111) and (001) were observed and found dominant at low and high deposition temperatures, respectively. However the reported temperature range in which the film orientation switches varies with the deposition technique: the lower the average energy of the depositing species, the higher the substrate temperature necessary to yield a dominant (001) Pt texture [7–9]. This suggests that the incident kinetic and subsequent thermal energies of the depositing species are

complementary regarding an energy threshold for the (001) Pt growth. The involvement of kinetic phenomena in the orientation development of the films has also been advanced. A decrease in the deposition rate has been reported [10] to cause a drastic lowering of the orientation switching temperature ($\approx$ 500 $\rightarrow$ 200 °C). A similar lowering ($\approx$ 500 $\rightarrow$ 350 °C) has also been obtained with seeded substrates [7].

The main objective of this research was to study the influence of the structural orientation of a Pt bottom electrode on the subsequent growth of SBN:*x* thin films deposited by R.F. magnetron sputtering. Two groups have published results about SBN thin films grown onto Pt coated MgO substrates [4, 11]. Both prepared SBN by using a sol-gel process and did not deal with the effect of the underlying Pt thin film characteristics on the SBN properties. The purpose of the work reported here was consequently three-fold: (1) control the orientation of Pt thin films deposited on (001) MgO in order to produce the Pt coated substrates necessary to the investigation, (2) study the possible evolution of this Pt orientation during deposition and crystallization of the SBN:*x* thin film, (3) examine the dependence of SBN:*x* growth characteristics on Pt crystallographic orientation. We used R.F. magnetron sputtering to prepare Pt and SBN:*x* thin films. Referring to the above mentioned results published [7, 10] about sputtered Pt thin films, we investigated the influence of substrate temperature, deposition rate, R.F. power, and seeding impurities on Pt orientation selection. Contrary to referred authors who varied the deposition rate by modifying the R.F. power, we varied the deposition rate by cancelling the magnetron effect, so that we were ensured to separate energetic from kinetic possible reasons for a change in the orientation, and to involve pure kinetic phenomena.

Experiment

Platinum and SBN:*x* thin films were deposited by using R.F. magnetron sputtering. The parameters of SBN:*x* deposition were fixed from the results of previous investigations [6, 12] in which we established the conditions for a stoichiometric deposit and for an epitaxial crystallization of the aimed tetragonal tungsten bronze SBN:*x* phase on (001) MgO substrates. Thin amorphous SBN films, about 0.6 μm thick, were deposited by RF magnetron sputtering of a polycrystalline target SBN: *x* (x = 48%), at 250 °C substrate temperature and 5×10^{-3} mbar plasma pressure (98% Ar + 2% O_2), on Pt coated (001) MgO substrates. The amorphous films were then crystallized at 800 °C by using halogen lamps.

In order to probe the influence of the deposition parameters on the Pt thin films orientation, we prepared three different targets by coating metallic discs 10 cm in diameter (Cu for target labelled 1, Fe for targets labelled 2 and 3) with platinum foils. The use of a Fe disc causes a deviation of the magnetic field lines, which are guided inside the disc. The magnetic field intensity at the surface of the platinum foil consequently collapses and the magnetron effect on the deposition rate is thus cancelled (Fig. 1). Target 3 differs from target 2 in that it is not perfectly coated with platinum thus allowing the co-sputtering of Fe atoms and the investigation of impurities influence on platinum growth. Thin Pt films, about 0.08 μm thick, were prepared from these three targets at 2×10^{-2} mbar Ar plasma pressure, on (001) MgO substrates. Substrates were heated using a resistive heater located inside the substrate block and regulated by a thermocouple labelled A (Fig. 2) close to the back face of the substrate. Figure 2 displays the deposition temperature measured by a second thermocouple labelled B in contact with the front surface to be coated with Pt, versus the back surface temperature. The initial difference between back and front surface temperatures is significant and due to the heat confinement inside the heater block. This difference increases with increasing platinum film thickness due to Pt mirror effect and increased heat confinement. According to the measurements plotted in Fig. 2, if we keep constant a back temperature of 700 °C, the deposition temperature varies from 434 to 334 °C between start and end of Pt deposition, thus making it difficult to define a deposition temperature of the film. As shown in the following, this deposition temperature is

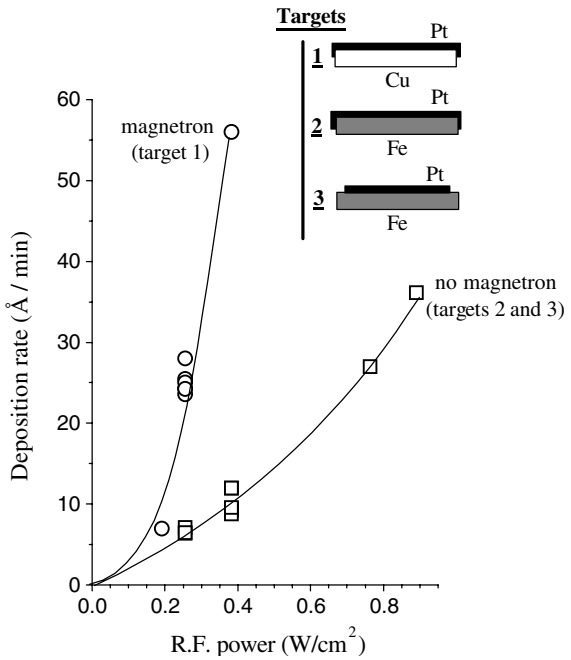

Fig. 1 Deposition rate of platinum films as a function of R.F. power with (target 1) and without (targets 2 and 3) magnetron effect

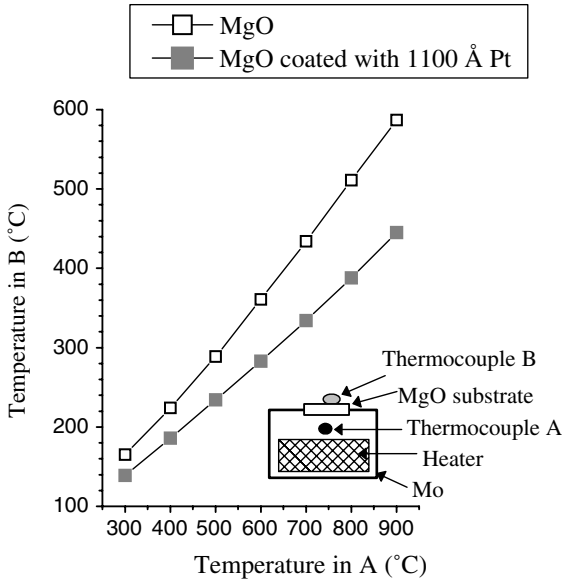

Fig. 2 Deposition temperature at the front surface of the MgO substrate as a function of the temperature measured on the back surface and used for regulation. The two cases of a Pt coated and a not Pt coated MgO substrate are shown

crucial for the orientation development of platinum. In order to maintain the surface temperature constant and unambiguously defined, we programmed an adjusted increase of the regulation back temperature during deposition.

Depending on its magnitude, the films thickness is determined from either spectrophotometry transmission or X-ray reflectometry measurements. X-ray (Cu $K_{\alpha 1}$) diffraction techniques (XRD) are used to identify crystalline structure and orientation.

Results and discussion

Orientation selection of Pt thin films on (001) MgO

As expected, a mixture of (111) and (001) oriented crystallites was observed in the Pt films we produced. From X-ray θ–2θ patterns of these films, we define the volume fraction of (111) oriented crystallites as A(111)/[A(111) + C × A(002)] where A(111) and A(002) are the integrated intensities of (111) and (002) reflections and C is a constant taking the respective structure factors into account (C = 1.57). This volume fraction is plotted as a function of deposition temperature in Fig. 3. A first experimental evidence is there is no significant effect of the deposition rate on the orientation switching temperature at fixed R.F. power: this switching temperature is found close to 470 °C whatever target we use (1 or 2) although the magnetron effect increases the deposition rate from 7 to 25 Å/min.

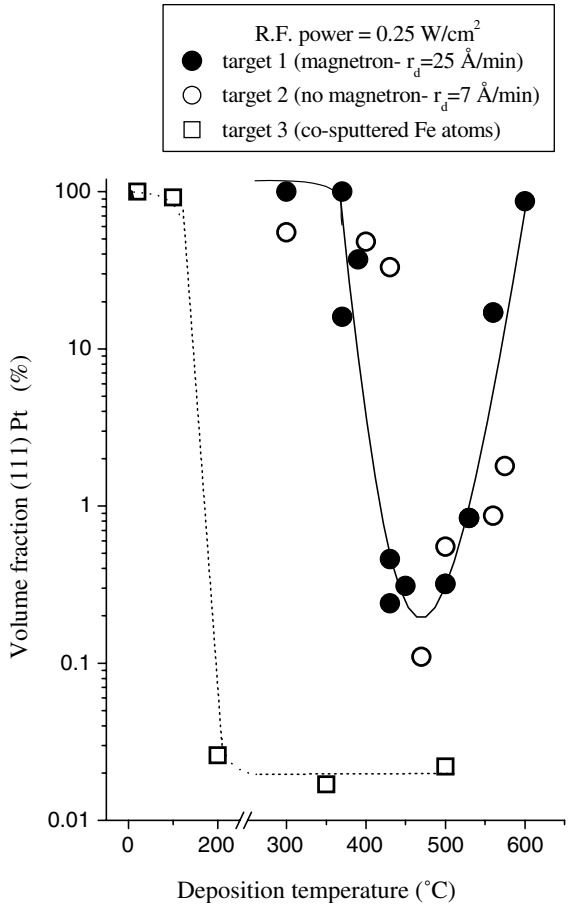

Fig. 3 Volume fraction of the (111) Pt crystallites in sputtered Pt thin films produced from the three different targets, as a function of the deposition temperature

This result suggests that the drastic decrease in orientation switching temperature reported by Ahn and Baik [10] (≈ 500 → ≈ 200 °C), and produced by a variation in R.F. power, should not be assigned to the correlated variation in deposition rate (≈ 54 → ≈ 36 Å/min) nor interpreted as a proof that kinetic phenomena play a leading role in the orientation development of Pt films.

We obtain the dominance of (001) orientation only in a narrow range of temperatures (470 ± 50 °C) while (111) orientation dominates not only at lower but also at higher temperatures. As illustrated in Fig. 4, this temperature range in which (001) orientation prevails slightly shifts towards lower temperatures (470 → 430 °C) and becomes narrower with increasing R.F. power (0.25 → 0.38 W/cm^2). This shift supports the interpretation in terms of an energetic threshold for the (001) Pt oriented growth, reached through complementary kinetic and thermal contributions.

The results obtained with target 3 (Fig. 3) indicate that Fe impurities drastically prevent the (111) oriented growth from 200 °C deposition temperature. This conclusion is

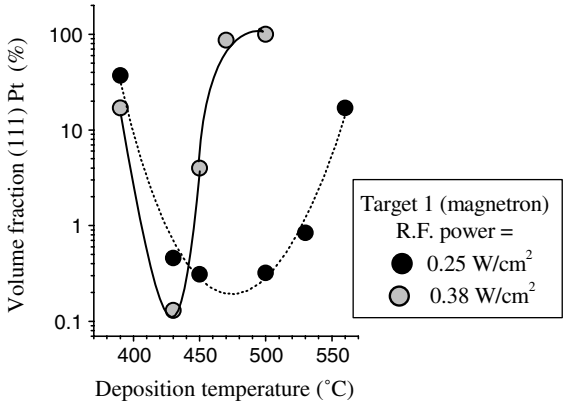

Fig. 4 Influence of R.F. power on the optimal temperature for (001) Pt orientation (films produced from target 1 with magnetron effect)

consistent with the above-mentioned [7] lowering of the orientation switching temperature obtained by using a sputtered Fe seed layer. This seed layer yielded (001) epitaxial films with no (111) material present down to the lowest temperature investigated by the authors (350 °C). We have tested that replacing Fe by Cu or Cr atoms yields a similar inhibition of the (111) Pt growth.

If deposition rate, as shown above, has no effect on the orientation switching temperature, we find it improves both surface roughness and (001) orientation quality of the Pt thin films. When increasing deposition rate from 7 to 25 Å/min by involving the magnetron effect (target 2 $\rightarrow$ target 1), RMS surface roughness varies from 9 to 3 Å while the rocking curve width for the (002) Pt peak decreases from 0.50 to 0.40°. Figure 5 illustrates the further improvement of this latter rocking curve width which results from an additional increase in deposition rate (25 $\rightarrow$ 56 Å/min) caused by R.F. power (0.25 $\rightarrow$ 0.38 W/cm^2). As shown in this figure, the second factor, which affects the rocking curve width is a deviation from the optimal conditions of (001) growth, represented by the (111) Pt volume fraction. The inset to Fig. 5 indicates that Fe impurities do not modify these optimal conditions, even though they inhibit the competitive (111) oriented Pt growth.

Whatever sputtering conditions we used, asymmetric X-ray diffraction scans from {220} Pt planes demonstrated that both populations of Pt crystallites have an epitaxial relationship with the MgO substrate. The (001) oriented Pt crystallites exhibit a cube-on-cube orientation (Fig. 6a) while the twelve reflections detected with a 30° separation between adjacent peaks (Fig. 6b) indicate a four-fold degeneracy of the in-plane alignment of (111) oriented Pt crystallites. The epitaxial orientation relationship is of the type [110] Pt//[110] MgO for both (001) Pt and (111) Pt on (001) MgO, identical to that found by all the authors who reported in the literature about epitaxial Pt thin films on

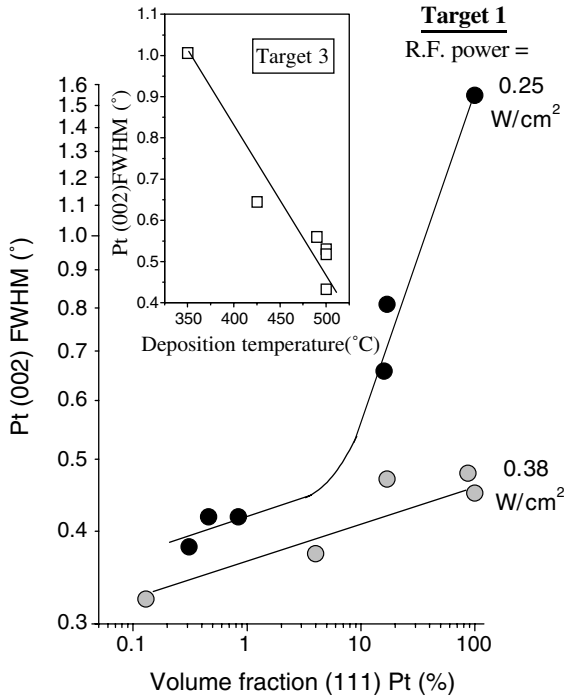

Fig. 5 (002) Pt rocking curve Full Width at Half Maximum (FWHM) as a function of (111) Pt volume fraction, which represents the deviation from optimal conditions for (001) Pt orientation. The two cases illustrated in this figure are those illustrated in Fig. 4 (target 1 and two different R.F. power values). The inset shows the dependence of the (002) Pt rocking curve width on deposition temperature in the case of Fe-contaminated Pt films

(001) MgO. Calculations have been carried out [13] which account for this result by assigning minima of the Pt/(001) MgO interface energy to these two experimental in-plane alignments.

The electrical resistivity of the Pt thin films we prepared is close to 12 μΩ · cm, to be compared to the bulk value of 10.6 μΩ · cm (at 20 °C).

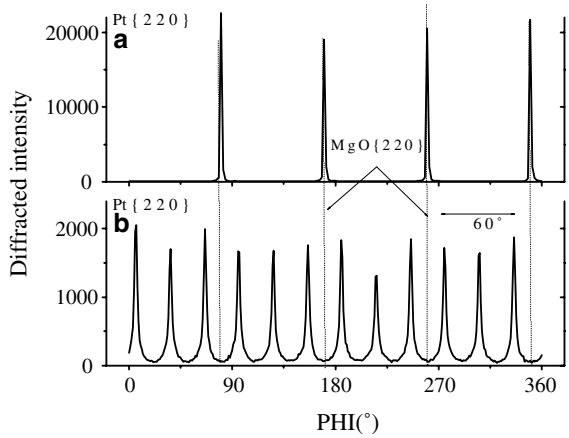

Fig. 6 Typical X-ray phi-scan measurements of the planes {220} obtained from (001) Pt crystallites (**a**) and (111) Pt crystallites (**b**)

Evolution of Pt orientation with subsequent annealing

Once characterized, Pt coated substrates have been introduced in the second sputtering chamber, coated with amorphous SBN under the above mentioned sputtering conditions, then annealed at 800 °C in order to crystallize the SBN deposit. A narrower width at half maximum of Pt reflection lines indicates that annealing causes a further coalescence of initial crystallites. The inferred crystallite size perpendicularly to the substrate is found close to the Pt film thickness. The evolution of Pt films orientation during this process, as deduced from post X-ray analysis, is shown in Fig. 7. Coalescence mechanisms unambiguously favour (111) orientation provided the initial volume fraction of (111) oriented Pt crystallites is higher than a very low threshold, around 0.1%. As a result, the deposition conditions which yield a stable dominant (001) Pt orientation under subsequent processing appear particularly critical. For clarity reasons, the case of Fe-contaminated thin films is not depicted in Fig. 7a. Annealing does not modify the dominant (001) orientation in these films, which may be consistently explained by a very low initial (111) volume fraction.

The evolution of the rocking curve with annealing is illustrated in Fig. 7b. Data relative to films prepared from the three targets, with the same fixed R.F. power (0.25 W/cm^2), have been plotted together. It appears that annealing improves the initial (001) Pt orientation quality regardless of the (001) and (111) volume fractions evolution. The initial rocking curve width and the annealing temperature (700 or 800 °C in Fig. 7b) determine the final rocking curve width. While a deposition temperature higher than about 500 °C causes a deterioration of the (002) Pt rocking curve width (see Figs. 5 and 7b), annealing temperatures as high as 700 or 800 °C cause its improvement. These contrasted roles played by temperature outline the difference between mechanisms involved in the two steps of the process. The achieved rocking curve width of 0.22° for the (002) Pt peak is among the best values reported before from any deposition technique.

We questioned the possible role of the top SBN film in these results by carrying out an identical annealing on Pt-coated substrates of varied (111) Pt volume fractions, and obtained results identical to the above ones, which establishes there is no influence of the SBN film presence on the Pt orientation evolution during annealing.

We also verified that annealing did not modify the in-plane alignment of (001) Pt or (111) Pt on (001) MgO.

Influence of Pt orientation on the subsequent growth of SBN

When prepared on (001) MgO substrates in the optimized sputtering and annealing conditions given above, the SBN

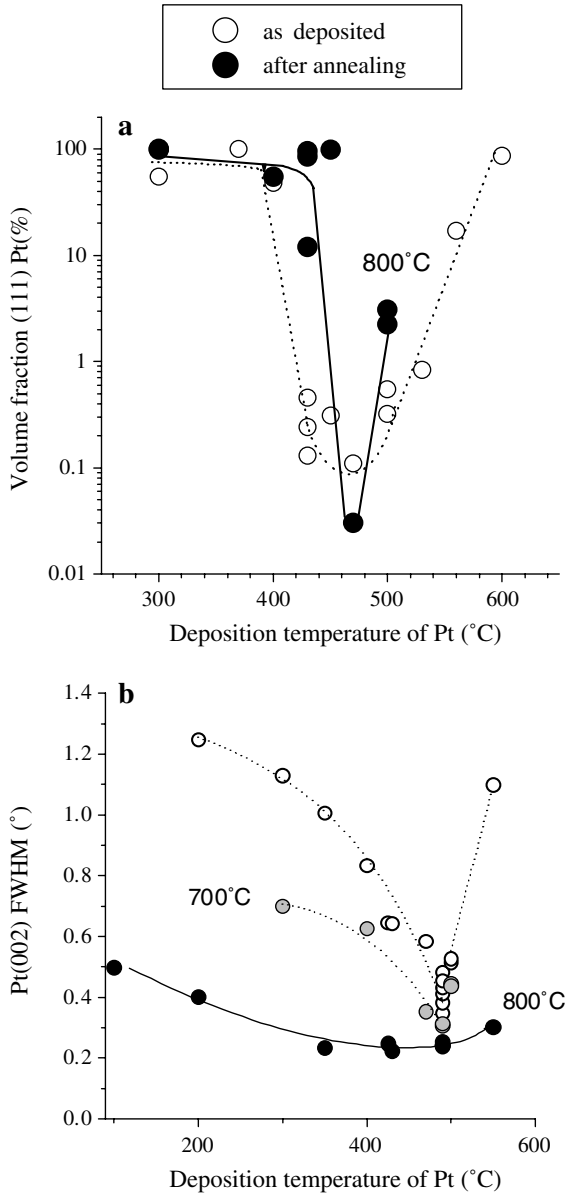

Fig. 7 Annealing of Pt films at a temperature sufficient to crystallise amorphous SBN: Evolution of the (111) Pt volume fraction (**a**) and (002) Pt rocking curve width (**b**) versus Pt deposition temperature

phase is (001) oriented, epitaxial, and displays only the two (001) and (002) SBN reflections in a symmetric X-ray scan (Fig. 8). The exact angular locations of the (001) and (002) SBN peaks depend on the Sr/Ba ratio due to the smaller size of Sr compared to Ba atom and to the subsequent variation in the lattice constants. The ratio of the order 1 to the order 2 intensities, r – 1/2, is lower than 1, as both predicted from simulation and observed in the X-ray patterns of the polycrystalline SBN targets. Due to the logarithmic scale used in Fig. 8, low intensity peaks appear alongside of the (001) and (002) SBN peaks. They have been unambiguously identified as issuing from the parasitic phase $SrNb_2O_6$, briefly noted SN (S for SrO and N for

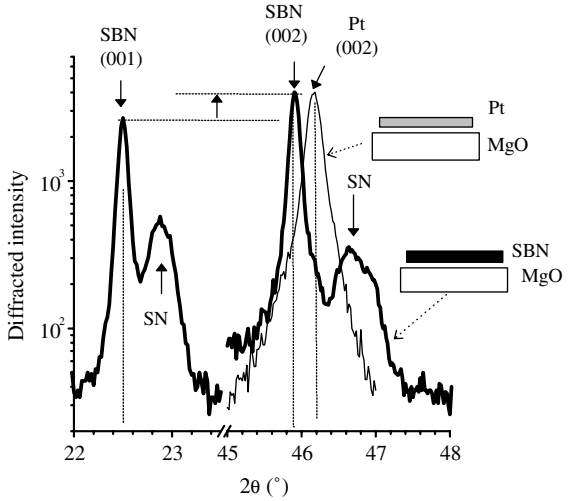

Fig. 8 Typical XRD θ–2θ scans of thin films sputtered on (001) MgO from a SBN:48 target, and from a Pt target. The two films are (001) oriented and the scans are shown only in the limited angular ranges around the corresponding reflections

Nb_2O_5). We have shown [12] that the SBN stoichiometry approach favours the epitaxial crystallization on (001) MgO of both SBN and SN, one at the expense of the other. The competing SN parasitic growth may be inhibited by using a sufficiently high crystallization temperature. In addition, Fig. 8 displays the (002) Pt reflection of a Pt film deposited on (001) MgO.

We have used the same optimized deposition and annealing conditions to prepare SBN thin films on Pt coated (001) MgO substrates. The (111) or (001) Pt dominant orientation was obtained by varying the Pt deposition temperature. Figures 9b and 10a show the X-ray symmetric patterns of two films simultaneously deposited and crystallized onto dominant (001) and (111) Pt, respectively. These spectra suggest a strong correlation between a (001) oriented SBN growth and the (001) orientation of underlying platinum. The integrated intensities of (001) SBN and (002) Pt reflections are found proportional: both are reduced to about 7% of their initial value from a spectrum to the other.

Moreover, these integrated intensities remain proportionally correlated when a further evolution of the (001) Pt volume fraction occurs. As discussed above, an annealing step may yield such an evolution. Figure 10b illustrates the simultaneous intensity decrease of the (001) SBN and (002) Pt reflections caused by a second annealing step after crystallization. These results allow to conclude that the (001) oriented growth of SBN on platinum is possible and occurs exclusively on (001) oriented Pt crystallites.

XRD phi-scans measured from (211) and (311) SBN planes further demonstrate that SBN is epitaxially grown on (001) Pt: the in-plane orientations deduced from these measurements are mirror symmetric (±18°) to the axis of the (001) Pt and (001) MgO cell axis. When directly grown on (001) MgO substrates, SBN displays also two mirror symmetric in-plane orientations but the angular rotation of the SBN cell relatively to MgO is ±31°. The fundamental reasons for these observed in-plane orientations, instead of a cube on cube orientation, are not easy to establish.

Conclusion

In the work reported here, the main question is the influence of the structural orientation of a Pt bottom electrode

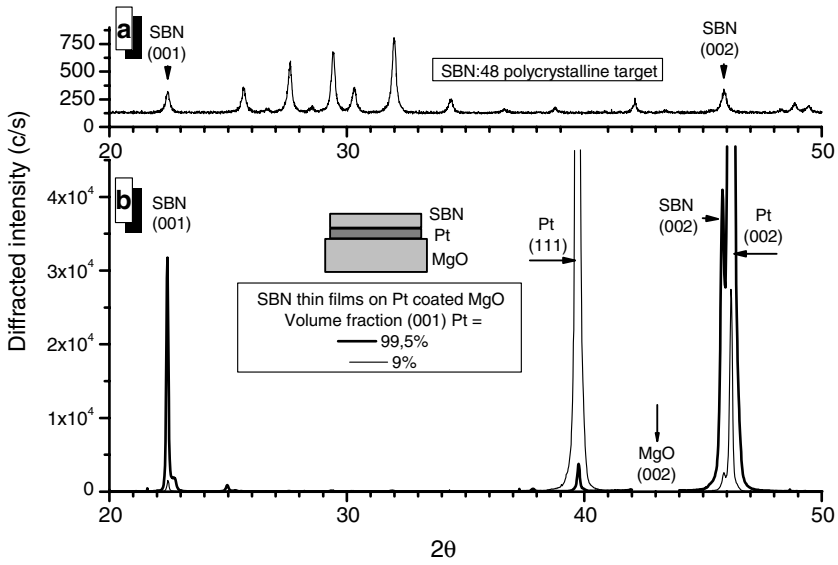

Fig. 9 Influence of Pt crystallographic orientation on subsequent SBN growth: **(a)** XRD θ–2θ scan of a polycrystalline SBN:48 target as reference (**b**) XRD θ–2θ scans of two films sputtered from the previous target, simultaneously deposited and crystallized on two Pt coated MgO substrates only different in the (001) Pt volume fraction (99.5% and 9%)

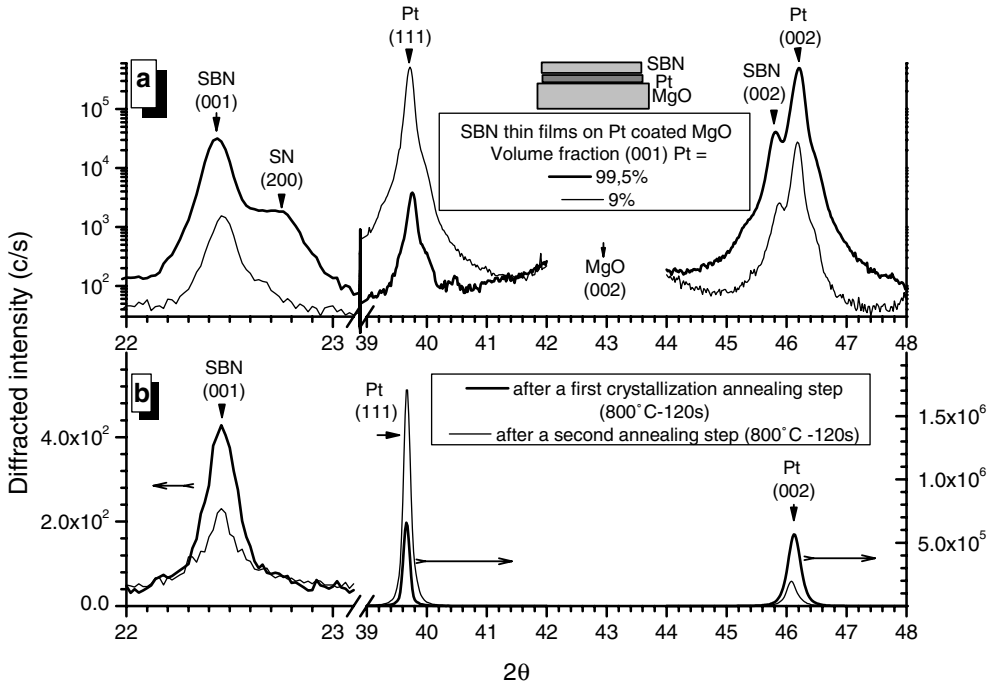

Fig. 10 (**a**) The XRD θ–2θ scans of Fig. 9b displayed with different scales (**b**) Evolution of the XRD θ–2θ scan of a SBN film grown on a Pt coated MgO substrate under a second annealing step (800 °C—120 s)

on the subsequent growth of SBN:x thin films deposited by R.F. magnetron sputtering, with electro-optic applications in view. It implies a prior control of the orientation of sputtered Pt films on (001) MgO substrates and the first part of this report is an additional contribution to the discussion about Pt orientation selection.

Our results lead us to draw the following conclusions: (1) The dominance of (001) Pt orientation is obtained in a narrow range of deposition temperatures, the location of which is between 400 and 500 °C, insensitive to deposition rate, sensitive to R.F. power, thus suggesting that kinetic phenomena are not involved in the orientation development of Pt films. Outside this temperature range, (111) orientation dominates. Both (001) and (111) crystallites populations exhibit an in-plane alignment of the type [110] Pt// [110] MgO. (2) Deposition rate is nevertheless not indifferent since it influences both Pt surface roughness and rocking curves width. (3) Impurities (Fe, Cu, Cr) inhibit the (111) Pt growth but don't modify the optimal temperature for (001) Pt growth. (4) Annealing at a temperature sufficient to crystallise the top SBN film causes a drastic evolution of the initial (111) and (001) Pt volume fractions, making particularly critical the deposition conditions for a final dominant (001) Pt texture on an unseeded substrate. (5) In these latter conditions, coalescence phenomena result in a single (001) Pt orientation and a rocking curve width as low as 0.22°. (6) The (001) oriented growth of SBN onto Pt coated MgO is possible but occurs exclusively on (001) oriented Pt crystallites. The SBN film is then epitaxial and displays two in-plane orientations mirror symmetric (±18°) to the axis of the underlying (001) Pt and (001) MgO cell axis. These in-plane orientations are different from those exhibited by SBN on MgO (±31°).

These conclusions indicate that platinum should be deposited on a seeded MgO substrate at the optimal temperature for (001) Pt growth and at high deposition rate. We expect this work will tend to an experimental demonstration of an electro-optic effect in sputtered SBN thin films.

References

1. Lu Z, Feigelson S, Route RK, Hiskes R, Dicarolis SA (1994) In Proceedings of the Metal-Organic-Chemical-Vapor-Deposition of Electronic Ceramics Symposium, Boston, November 1993, edited by the Mat. Res. Soc., vol. 335, Pittsburgh, p. 59
2. Schwyn Thöny S, Youden KE, Harris JS Jr, Hesselink L (1994) Appl Phys Lett 65:2018
3. Zhu LD et al. (1995) Appl Phys Lett 67:1836
4. Sakamoto W, Yogo T, Kikuta K, Kawase A, Hirano S (1996) J Am Ceram Soc 79:2283
5. Li AD, Mak CL, Wong KH, Wu D, Ming NB (2001) J Mater Res 16:3179

6. Cuniot-Ponsard M, Desvignes JM, Ea-Kim B, Leroy E (2003) J Appl Phys 93:1718
7. Lairson BM, Visokay MR, Sinclair R, Hagstrom S, Clemens BM (1992) Appl Phys Lett 61:1390
8. Narayan J, Tiwari P, Jagannadham K, Holland OW (1994) Appl Phys Lett 64:2093
9. McIntyre PC, Maggiore CJ, Nastasi M (1995) J Appl Phys 77:6201
10. Ahn KH, Baik S (2002) J Mater Res 17:2334
11. Koo J, JH Jang, B-S Bae (2000) J Sol-Gel Sci Technol 19:611
12. Cuniot-Ponsard M, Desvignes JM, Leroy E (2003) Ferroelectrics 288:159
13. McIntyre PC, Maggiore CJ, Nastasi M (1997) Acta mater 45:869